

Recent update of the XRT response. III. Effective Area – Update of relative normalization among XIS0-3 and PIN –

Yoshitomo MAEDA, Kentaro SOMEYA, Manabu ISHIDA, and the XRT team
Kiyoshi HAYASHIDA, Hideyuki MORI, and the XIS team
e-mail:ymaeda@astro.isas.jaxa.jp

July 15, 2008

1 Overview

In this document, we present an update of relative normalizations of XIS0 through 3 and HXD PIN reported on a suzakumemo JX-ISAS-SUZAKU-MEMO-2007-11. The update was necessary because the major change was made for the arf generator (xissimarfgen/xissim) and for its calibration files (CALDB 20080709). The version of the arf builder `xissimarfgen` is 2008-04-05. This arf builder must be used with a combination of the rmf file that is made with the recent XIS CALDB 20080709.

The following versions of the data, software or CALDB were adopted in this memo.

- Data: V2.1. The empirical correction of sky coordinates of X-ray photons by Uchiyama et al. 2008 was applied.
- xissim or xissimarfgen version 2008-04-05
- xisrmfgen version 2007-05-14
- CALDB 20080709

The effective area of the XRT-XIS system is included in the arf and rmf files separately. The arf and rmf files are produced with the xissimarfgen and xisrmfgen software, respectively. The transmissivity of the XRT thermal shield and the effective area of the reflectors are included in the arf file. The transmissivity of the contamination onto the XIS optical blocking filter (OBF) is also included in the arf file while the detection efficiency of the XIS (the OBF transmissivity and the quantum efficiency) is contained in the rmf file. Our recent update was made both for the response of the mirror and for the detection efficiency of the detector. This is the reason why we need to regenerate both ARFs and RMFs by running the xissimarfgen or the xisrmfgen using the updated CALDB files. The quantitative summary of the updates of the XRT effective area and the XIS detection efficiency was summarized in Appendix A. Note that no change on the low-energy transmissivity of the thermal shield or the OBF was made. Therefore, no response function below 1 keV was changed.

In the following section, we summarize the power-law fits to the Crab spectra, a standard candle of the effective area confirmation. The detail method of the data reduction and analysis is the same as we gave in the suzakumemo JX-ISAS-SUZAKU-MEMO-2007-11.

The results of the XIS nominal and HXD nominal pointing positions are summarized in § 2 and § 3, respectively. Each section consists of (1) the spectral parameters of individual detectors, (2) the power-law normalizations when the photon index is constrained to be the same, and (3) their variation when the PIN energy band used in fitting is changed.

Photon index from each detector ... Photon-index of the XIS is in the range 2.07–2.09 and 2.07–2.11 at the XIS and HXD nominal positions (table 1 and table 4), respectively. That of the PIN is 2.09–2.10. No big change was found due to this update.

Relative normalization of each detector ... Normalization factor "const" relative to that of XIS0 is in the range 0.99–1.03 and 1.01–1.06 at the XIS and HXD nominal positions (table 2 and table 5), respectively. That of the PIN is 1.16–1.17. Note that the flux of the XIS-0 and -1 at the HXD nominal position is significantly changed at this version. This is because the vignetting function of the XRTs was slightly improved (JX-ISAS-SUZAKU-MEMO-2008-05).

Absolute normalization of each detector ... The 2–10 keV flux of the Crab ranges 2.09–2.14 and $2.03\text{--}2.16 \times 10^{-8}$ erg cm⁻²s⁻¹ at the XIS and HXD nominals, respectively (table 1 and table 4). The flux at the XIS nominal position is ~3–5% smaller than that reported using the previous response files (JX-ISAS-SUZAKU-MEMO-2007-11).

In this memo, we report reproducibility on the effective area for the combination of the recent software and the CALDB 20080709. Calibration reports on the image and the vignetting function of the XRTs is presented in the other companion memos (Image:JX-ISAS-SUZAKU- MEMO-2008-04, Vignetting:05).

References

- [1] Serlemitsos et al. 2007, PASJ **59**, 9

2 XIS nominal position

2.1 Independent Fit

Table 1: Power-law fit to individual XIS and PIN spectra at the XIS nominal position. Used energy bands are XIS:1.0–1.6 1.9–10keV and PIN:12–40keV.

Detector	N_{H} [10^{22}cm^{-2}]	Γ	Norm ^a	Flux ^b	χ^2_{ν} (dof)
XIS0	0.311 ± 0.015	2.077 ± 0.017	$9.38^{+0.24}_{-0.23}$	2.086	1.02 (89)
XIS1	0.294 ± 0.014	2.085 ± 0.017	$9.73^{+0.23}_{-0.22}$	2.141	1.59 (89)
XIS2	0.282 ± 0.015	2.065 ± 0.017	$9.29^{+0.23}_{-0.22}$	2.134	1.34 (89)
XIS3	0.304 ± 0.015	2.082 ± 0.017	$9.33^{+0.24}_{-0.23}$	2.062	1.34 (89)
PIN	0.3 (fix)	2.101 ± 0.008	11.41 ± 0.26	2.464	0.74 (72)

a: photons $\text{cm}^{-2}\text{s}^{-1}\text{keV}^{-1}$ at 1 keV.

b: $10^{-8}\text{erg cm}^{-2}\text{s}^{-1}$ in 2–10 keV.

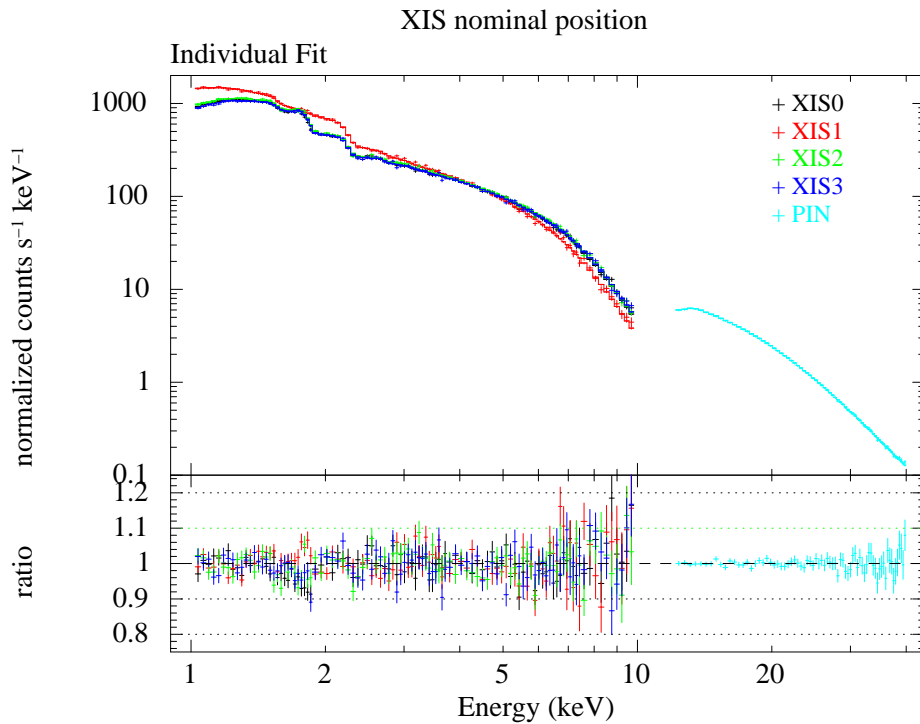


Figure 1: Power-law fit to individual XIS and PIN spectra at the XIS nominal position.

2.2 Fit with Common Γ

2.2.1 with all XIS modules

Table 2: Power-law fit with a common photon index to all XIS and PIN spectra at the XIS nominal position. Used energy bands are XIS:1.0–1.6 1.9–10keV and PIN:12–40keV.

Detector	N_{H} [10^{22}cm^{-2}]	Γ	const	Norm ^a	Flux ^b	χ^2_{ν} (dof)
XIS0	0.321 ± 0.009	2.090 ± 0.006	1.000 (fix)	9.55 ± 0.10	2.080	1.24 (432)
XIS1	0.298 ± 0.008		1.025 ± 0.010			
XIS2	0.302 ± 0.008		1.018 ± 0.010			
XIS3	0.311 ± 0.009		0.988 ± 0.010			
PIN	0.3 (fix)		1.158 ± 0.013			

a: photons $\text{cm}^{-2}\text{s}^{-1}\text{keV}^{-1}$ at 1 keV.

b: $10^{-8}\text{erg cm}^{-2}\text{s}^{-1}$ in 2–10 keV.

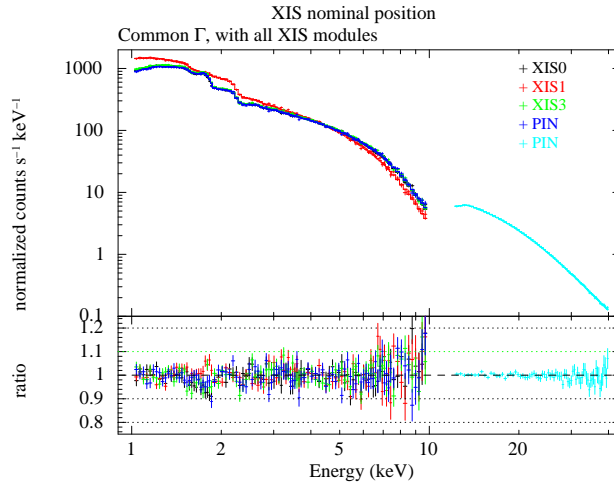


Figure 2: Power-law fit to all XIS and PIN spectra with a common photon index.

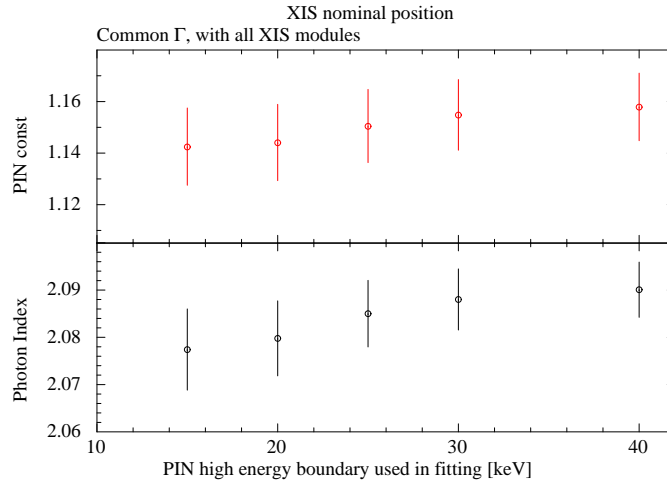


Figure 3: PIN normalization relative to that of XIS0 and photon index as a function of the PIN high energy boundary used in fitting.

2.2.2 without XIS2

Table 3: Power-law fit with a common photon index to XIS0, 1, 3 and PIN spectra at the XIS nominal position. Used energy bands are XIS:1.0–1.6 1.9–10keV and PIN:12-40keV.

Detector	N_{H} [10^{22}cm^{-2}]	Γ	const	Norm ^a	Flux ^b	χ^2_{ν} (dof)
XIS0	0.324 ± 0.009	2.094 ± 0.006	1.000 (fix)	$9.59^{+0.11}_{-0.10}$	2.079	1.20 (342)
XIS1	0.300 ± 0.008		1.025 ± 0.010			
XIS3	0.313 ± 0.009		0.988 ± 0.010			
PIN	0.3 (fix)		1.164 ± 0.014			

a: photons $\text{cm}^{-2} \text{s}^{-1} \text{keV}^{-1}$ at 1 keV.

b: $10^{-8} \text{erg cm}^{-2} \text{s}^{-1}$ in 2-10 keV.

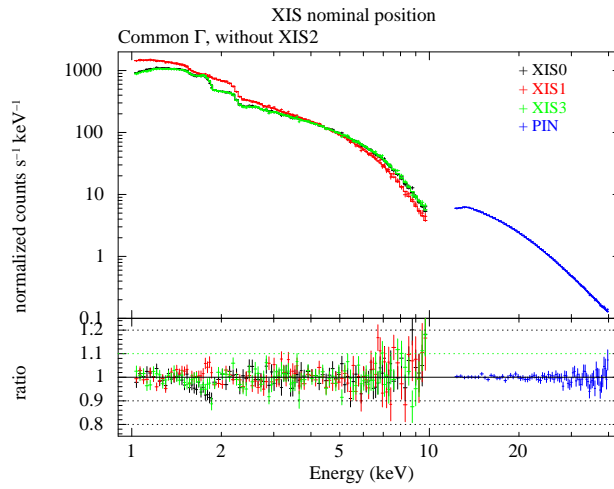


Figure 4: Power-law fit to XIS0, 1, 3 and PIN spectra with a common photon index.

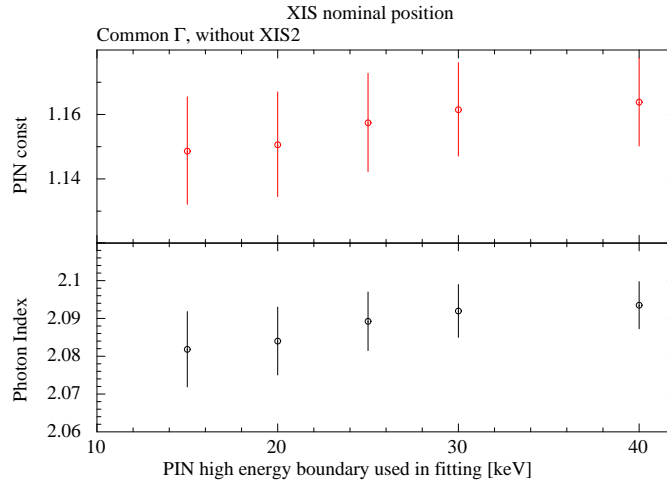


Figure 5: PIN normalization relative to that of XIS0 and photon index as a function of the PIN high energy boundary used in fitting.

3 HXD nominal position

3.1 Independent Fit

Table 4: Power-law fit to individual XIS and PIN spectra at the HXD nominal position. Used energy bands are XIS:1.0–1.6 1.9–10keV and PIN:12–40keV.

Detector	N_{H} [10^{22}cm^{-2}]	Γ	Norm ^a	Flux ^b	χ^2_{ν} (dof)
XIS0	0.304 ± 0.018	2.079 ± 0.021	$9.13^{+0.27}_{-0.26}$	2.025	1.28 (89)
XIS1	0.295 ± 0.016	2.111 ± 0.021	$9.59^{+0.27}_{-0.26}$	2.030	0.86 (89)
XIS2	0.282 ± 0.016	2.070 ± 0.019	$9.54^{+0.26}_{-0.25}$	2.151	1.22 (89)
XIS3	$0.301^{+0.017}_{-0.016}$	2.085 ± 0.019	9.29 ± 0.25	2.043	1.19 (89)
PIN	0.3 (fix)	2.090 ± 0.009	10.93 ± 0.27	2.400	0.82 (72)

a: photons $\text{cm}^{-2}\text{s}^{-1}\text{keV}^{-1}$ at 1 keV.

b: $10^{-8}\text{erg cm}^{-2}\text{s}^{-1}$ in 2–10 keV.

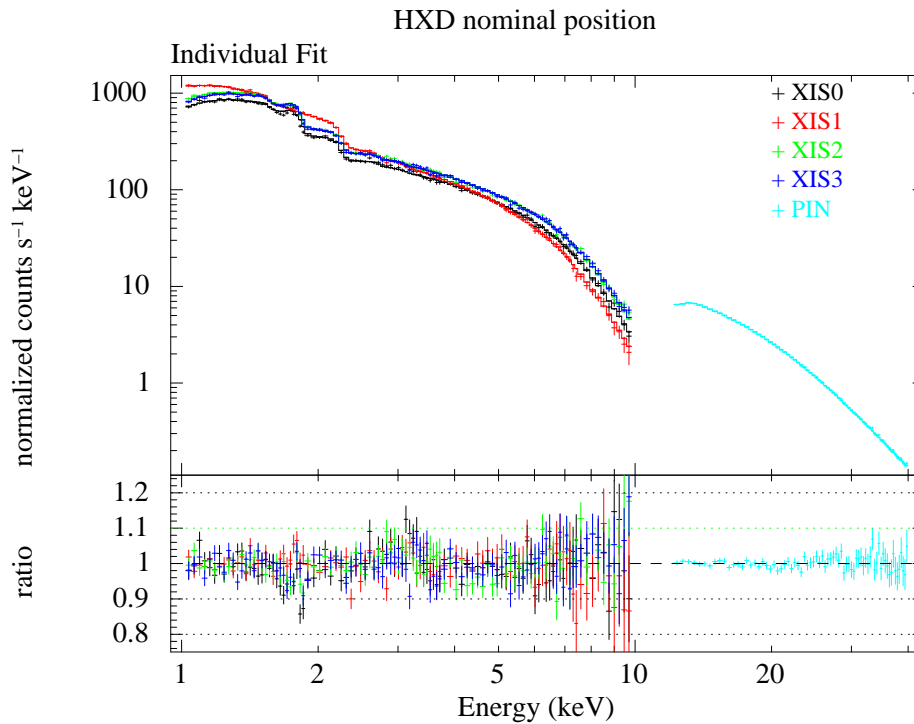


Figure 6: Power-law fit to individual XIS and PIN spectra at the HXD nominal position.

3.2 Fit with Common Γ

3.2.1 with all XIS modules

Table 5: Power-law fit with a common photon index to all XIS and PIN spectra at the HXD nominal position. Used energy bands are XIS:1.0–1.6 1.9–10keV and PIN:12–40keV.

Detector	N_{H} [10^{22}cm^{-2}]	Γ	const	Norm ^a	Flux ^b	χ^2_{ν} (dof)
XIS0	0.307 ± 0.011	2.086 ± 0.007	1.000 (fix)	$9.19^{+0.12}_{-0.11}$	2.019	1.13 (432)
XIS1	0.277 ± 0.009		1.010 ± 0.011			
XIS2	0.298 ± 0.010		1.060 ± 0.012			
XIS3	0.300 ± 0.010		1.010 ± 0.011			
PIN	0.3 (fix)		1.175 ± 0.015			

a: photons $\text{cm}^{-2}\text{s}^{-1}\text{keV}^{-1}$ at 1 keV.

b: $10^{-8}\text{erg cm}^{-2}\text{s}^{-1}$ in 2–10 keV.

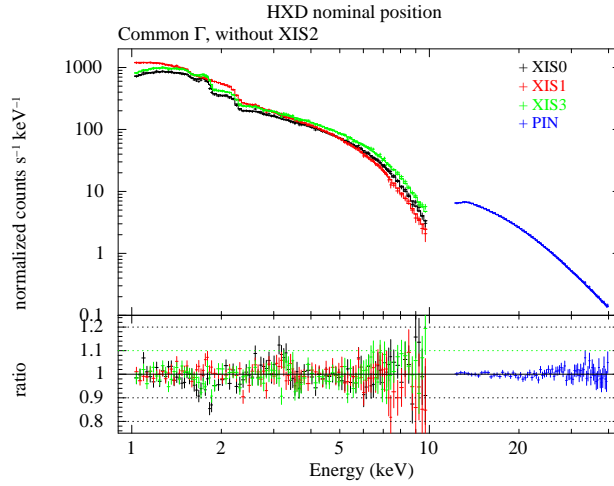


Figure 7: Power-law fit to all XIS and PIN spectra with a common photon index.

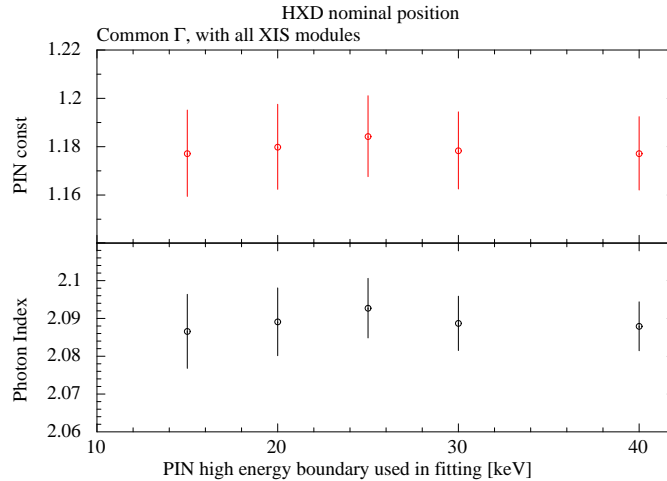


Figure 8: PIN normalization relative to that of XIS0 and photon index as a function of the PIN high energy boundary used in fitting.

3.2.2 without XIS2

Table 6: Power-law fit with a common photon index to XIS0, 1, 3 and PIN spectra at the HXD nominal position. Used energy bands are XIS:1.0–1.6 1.9–10keV and PIN:12-40keV.

Detector	N_{H} [10^{22}cm^{-2}]	Γ	const	Norm ^a	Flux ^b	χ^2_{ν} (dof)
XIS0	0.312 ± 0.010	2.090 ± 0.007	1.000 (fix)	9.27 ± 0.11	2.020	1.05 (342)
XIS1	0.280 ± 0.009		1.007 ± 0.011			
XIS3	0.305 ± 0.009		1.009 ± 0.011			
PIN	0.3 (fix)		1.181 ± 0.016			

a: photons $\text{cm}^{-2}\text{s}^{-1}\text{keV}^{-1}$ at 1 keV.

b: $10^{-8}\text{erg cm}^{-2}\text{s}^{-1}$ in 2-10 keV.

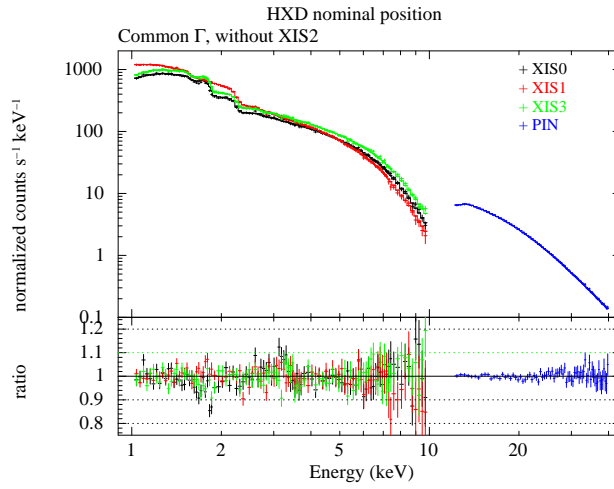


Figure 9: Power-law fit to XIS0, 1, 3 and PIN spectra with a common photon index at the HXD nominal position.

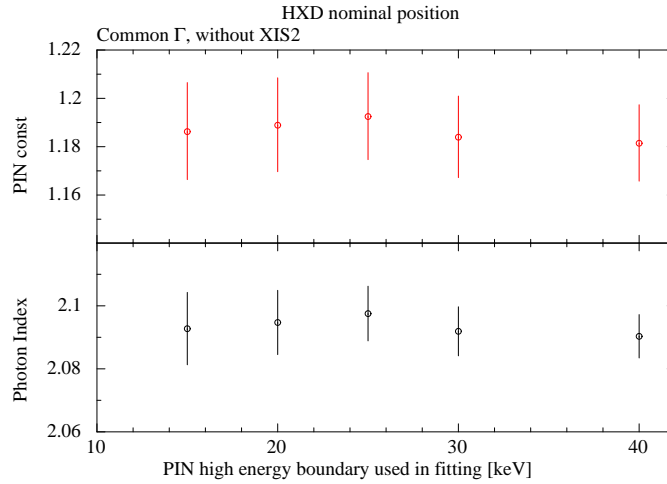


Figure 10: PIN normalization relative to that of XIS0 and photon index as a function of the PIN high energy boundary used in fitting.

Appendix A. XRT effective area and XIS detection efficiency

The new response is made using the CALDB 20060709. The old (and previous) was made with the CALDB 20080401 or earlier and was used in the suzakupmemo JX-ISAS-SUZAKU-MEMO-2007-11. Note that the XRT effective area is not calculated at the optical axis of the XRT but at the xis nominal position of the satellite pointing. A small modification around the Si-edge structure (XAFS) was made only for the XIS0.

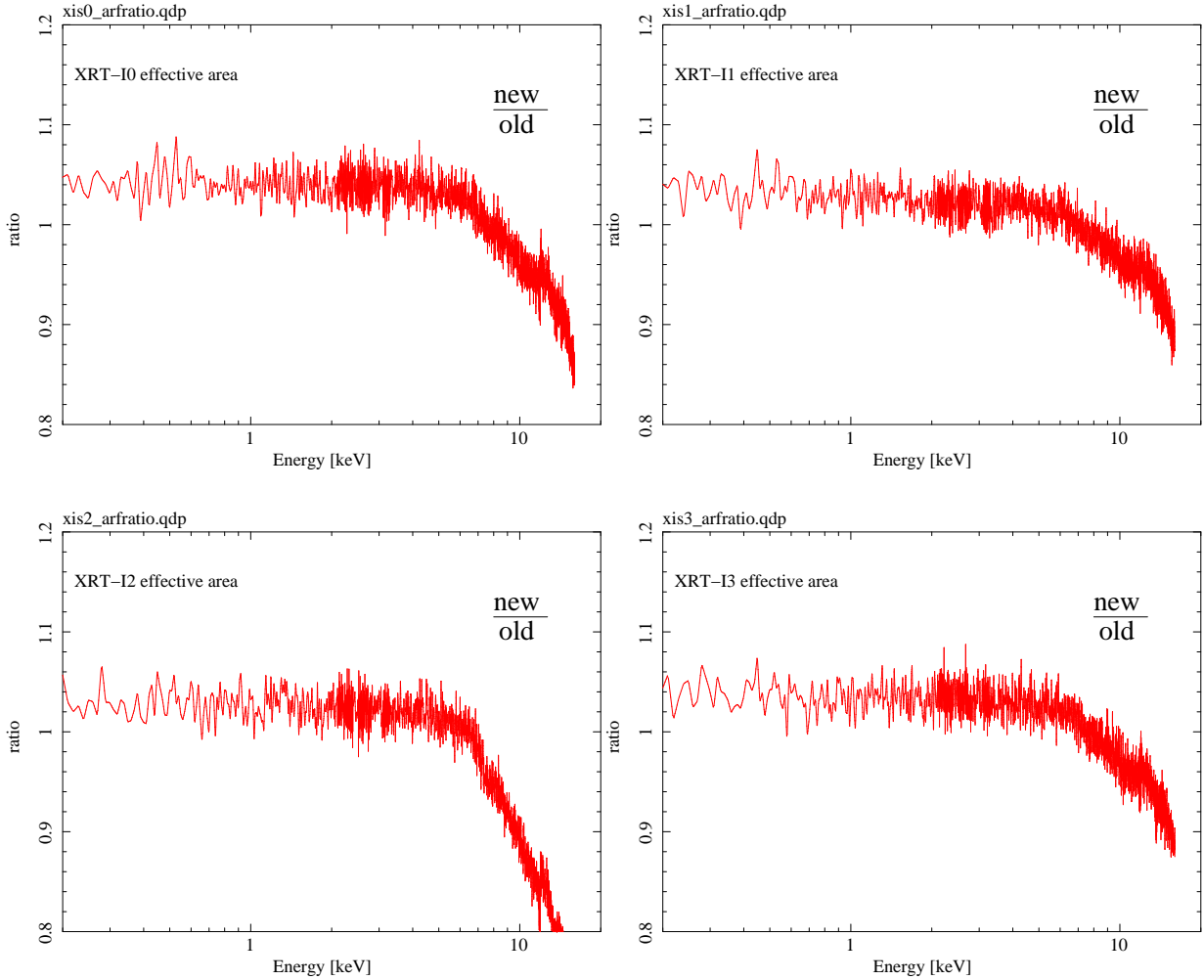


Figure 11: Ratios of the effective area of the XRTs.

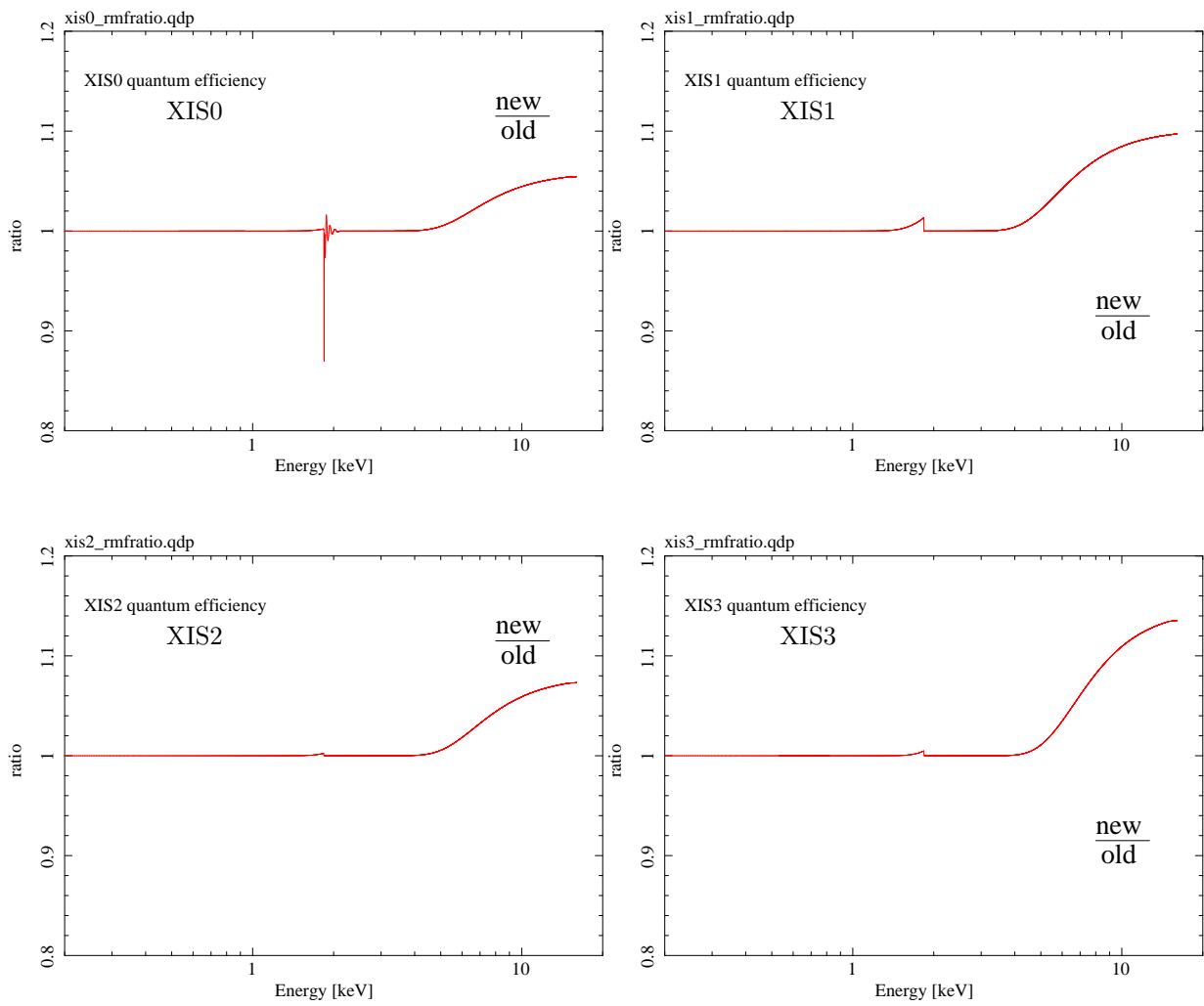


Figure 12: Ratios of the quantum efficiency of the XISs.

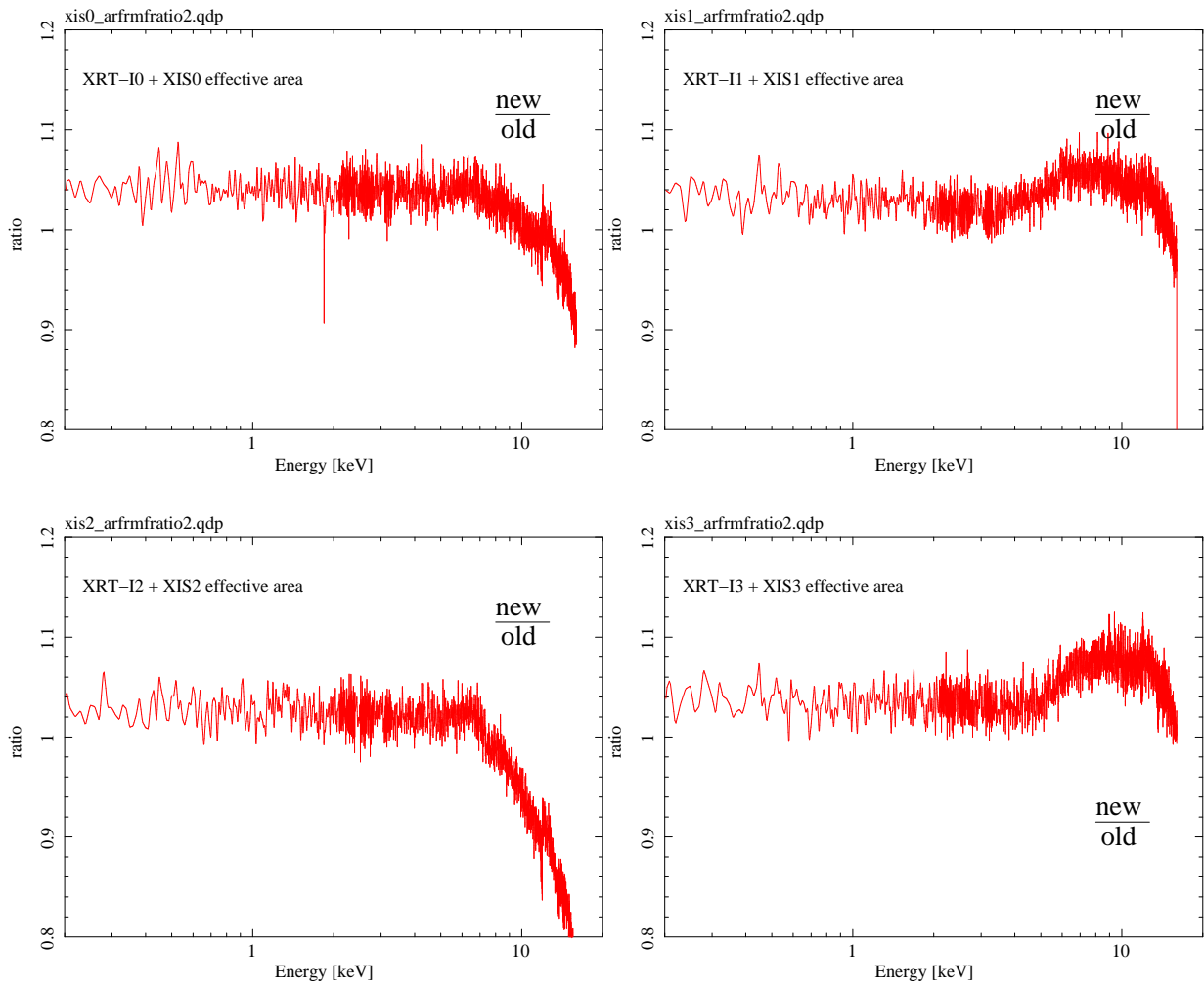


Figure 13: Ratios between the new and old effective area for the combination of the XRTs/XISs system.

Appendix B. Photon index of the Crab nebula

The best-fit parameters of the single power-law model is slightly different to the energy boundary used in fitting. We summarize the best-fit photon index when we change the energy boundary of interest around 1.5–2.0 keV.

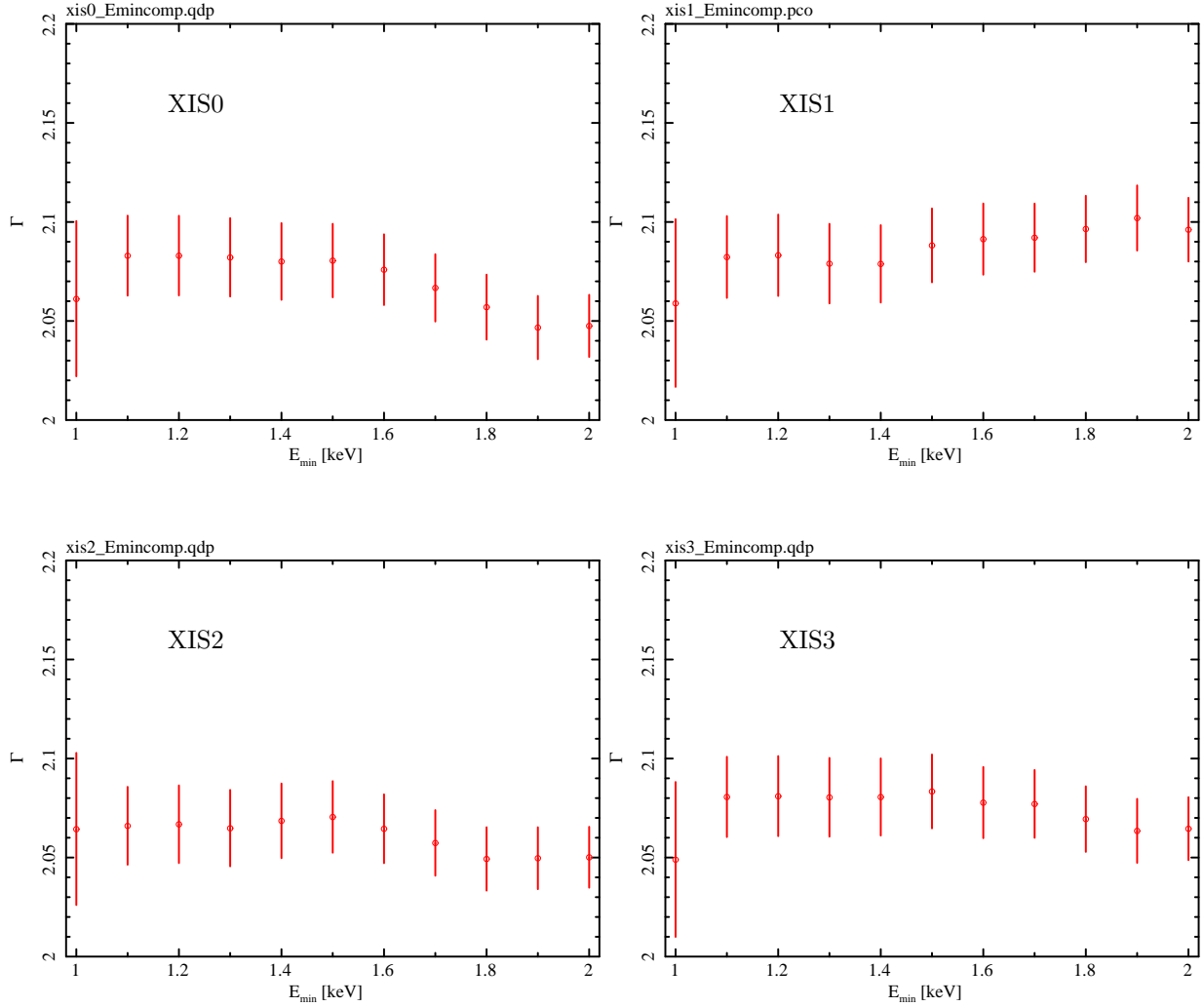


Figure 14: Best-fit photon index of the XISs. The horizontal axis corresponds to the lower energy band (E_{\min}) excluded in the spectral fit. The maximum energy band excluded is 2.0 keV. The energy band we used is then 1.0– E_{\min} and 2.0–10.0 keV.

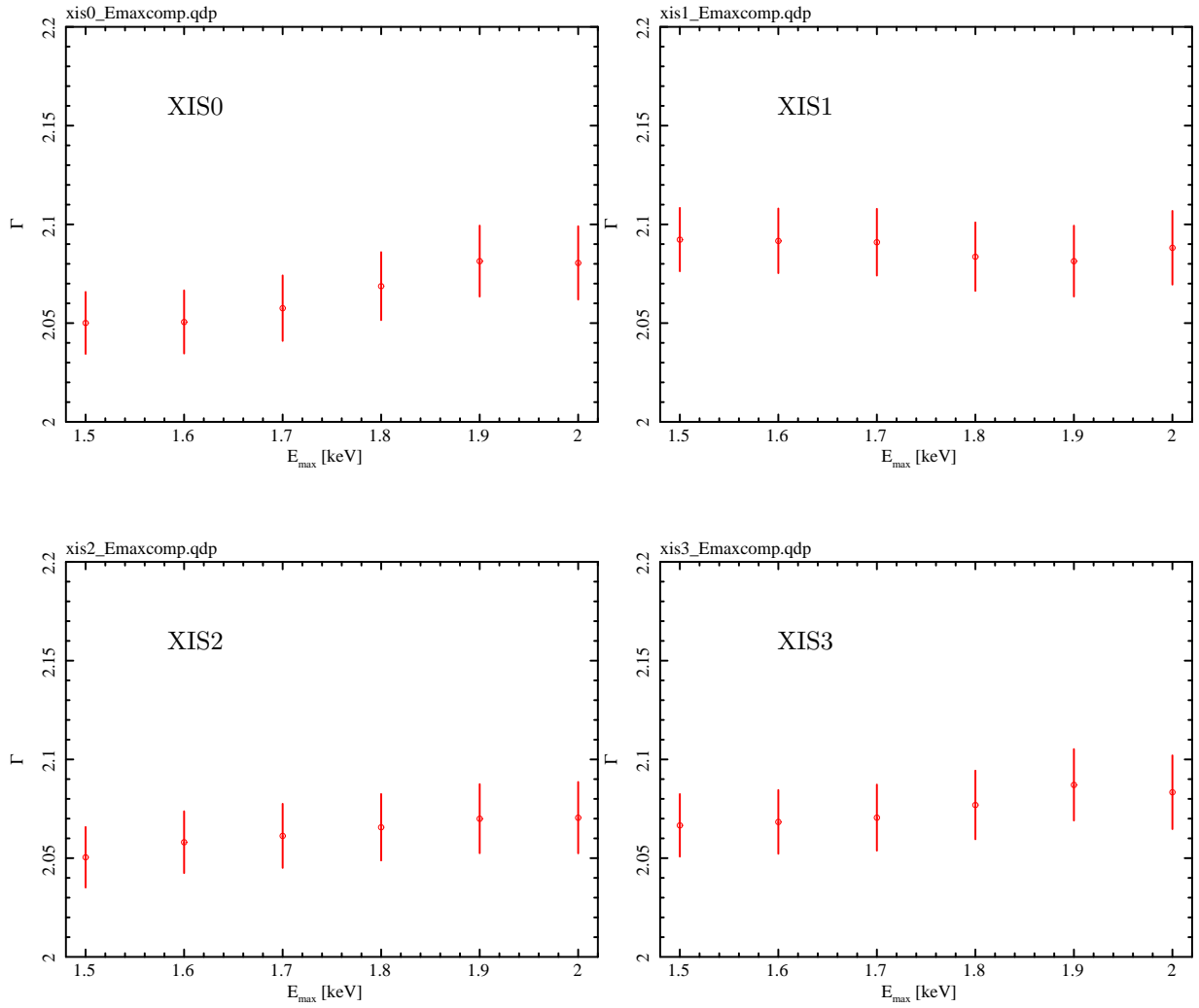


Figure 15: Best-fit photon index of the XISs. The horizontal axis corresponds to the lower energy band excluded in the spectral fit. The maximum energy band excluded is 1.5 keV. The energy band we used is then 1.0–1.5 and E_{\max} –10.0 keV.